

An In Vitro Protocol for Recording From Spinal Motoneurons of Adult Rats

Jonathan S. Carp,^{1,2} Ann M. Tennissen,¹ Donna L. Mongeluzi,¹ Christopher J. Dudek,¹ Xiang Yang Chen,^{1,2} and Jonathan R. Wolpaw^{1,2}

¹Wadsworth Center, New York State Department of Health, and ²Department of Biomedical Sciences, School of Public Health, State University of New York at Albany, Albany, New York

Submitted 31 March 2008; accepted in final form 30 April 2008

Carp JS, Tennissen AM, Mongeluzi DL, Dudek CJ, Chen XY, Wolpaw JR. An in vitro protocol for recording from spinal motoneurons of adult rats. *J Neurophysiol* 100: 474–481, 2008. First published May 7, 2008; doi:10.1152/jn.90422.2008. In vitro slice preparations of CNS tissue are invaluable for studying neuronal function. However, up to now, slice protocols for adult mammalian spinal motoneurons—the final common pathway for motor behaviors—have been available for only limited portions of the spinal cord. In most cases, these preparations have not been productive due to the poor viability of motoneurons in vitro. This report describes and validates a new slice protocol that for the first time provides reliable intracellular recordings from lumbar motoneurons of adult rats. The key features of this protocol are: preexposure to 100% oxygen; laminectomy prior to perfusion; anesthesia with ketamine/xylazine; embedding the spinal cord in agar prior to slicing; and, most important, brief incubation of spinal cord slices in a 30% solution of polyethylene glycol to promote resealing of the many motoneuron dendrites cut during sectioning. Together, these new features produce successful recordings in 76% of the experiments and an average action potential amplitude of 76 mV. Motoneuron properties measured in this new slice preparation (i.e., voltage and current thresholds for action potential initiation, input resistance, afterhyperpolarization size and duration, and onset and offset firing rates during current ramps) are comparable to those recorded in vivo. Given the mechanical stability and precise control over the extracellular environment afforded by an in vitro preparation, this new protocol can greatly facilitate electrophysiological and pharmacological study of these uniquely important neurons and other delicate neuronal populations in adult mammals.

INTRODUCTION

Spinal motoneurons were the first central mammalian neurons studied with intracellular electrodes (Brock et al. 1951). Their study has provided the basis for much of what is known about intrinsic neuronal properties and synaptic transmission (Brownstone 2006; Burke 1981, 2006). Furthermore, spinal motoneurons—particularly lumbar and cervical motoneurons—play a central role in motor control as integrators of synaptic input and encoders of motor commands.

Understanding of the essential role of spinal motoneurons would be greatly benefited by acquiring knowledge of their intrinsic properties through the use of in vitro preparations from adult animals. In vitro preparations are widely used in physiological and pharmacological studies of mammalian CNS neurons (Berger 1990; Dingleline et al. 1980; Dunwiddie et al. 1983) because they provide better access, mechanical stability, and control over the extracellular environment than do in vivo preparations. In vitro preparations of immature mammalian

spinal cord can provide excellent motoneuron recordings, but suffer from the limitation that the developmental status of the spinal circuitry is different from that in the adult (Biscoe and Duchon 1986; Jiang et al. 1999; Kerkut and Bagust 1995; Reklung et al. 2000). Application of in vitro methodology to the study of spinal motoneurons from adult mammals has had only limited success. The sacrocaudal spinal cord of adult rats affords reliable motoneuron recordings (Bennett et al. 2001), but is not directly relevant to limb motor control. Some in vitro recordings of cervical motoneurons from adult rodents have been reported (Hori et al. 2001, 2002), but in vitro preparations of lumbar spinal cord with viable motoneurons have proven to be more difficult. A brief report described a small number of recordings from the isolated lumbar spinal cord of the mouse (Fulton 1986), but further studies with that method were not forthcoming. Our own efforts to develop lumbar spinal cord slices using the methodology described for cervical slices (Hori et al. 2001) produced only a few successful recordings (Carp et al. 2003).

The lack of success with in vitro preparations of lumbar spinal cord from adult mammals is largely attributable to two factors: tissue hypoxia/ischemia and mechanical damage. Spinal motoneurons are very sensitive to ischemia and other insults (Carriedo et al. 1996; Nohda et al. 2007; von Lewinski and Keller 2005). Lumbar motoneurons appear to be especially sensitive (Duggal and Lach 2002), which is consistent with their poor viability in vitro (Bagust and Kerkut 1981). In vitro method development to date has focused on rapid cooling to minimize hypoxic and ischemic damage and on using glutamate antagonists or modifications of the extracellular solution to reduce neuronal firing and concomitant excitotoxicity (Bennett et al. 2001; Carlin et al. 2000; Hori et al. 2001, 2002).

Although these methods are beneficial, they do not address the mechanical damage that is incurred during tissue preparation. The spinal cord is fragile and easily damaged; dissection techniques try to minimize this damage (e.g., Hori et al. 2001). What has not been addressed previously is the massive damage that sectioning causes by transecting a neuron's dendrites (Davies et al. 2007). This is particularly severe for spinal motoneurons, which have large cell bodies (e.g., 35- μ m average diameter in rats) and elaborate dendritic fields that can extend out 1–2 mm from the soma and constitute \geq 96% of their surface area (Chen and Wolpaw 1994; Ulfhake and Kellerth 1981). The many breaches of the motoneuron membrane produced by dendritic amputations are probably a major

Address for reprint requests and other correspondence: J. S. Carp, Wadsworth Center, New York State Department of Health, PO Box 509, Albany, NY 12201-0509 (E-mail: carpj@wadsworth.org).

The costs of publication of this article were defrayed in part by the payment of page charges. The article must therefore be hereby marked "advertisement" in accordance with 18 U.S.C. Section 1734 solely to indicate this fact.

reason for the poor viability of motoneurons in slice preparations.

Polyethylene glycol (PEG) induces rapid refusion of severed peripheral and central axons (Lore et al. 1999; Shi et al. 1999). We hypothesized that PEG could also reseal the dendritic processes that are cut during sectioning and could thereby substantially improve motoneuron viability. This study assesses the impact of PEG and other methodological changes that minimize ischemia and maximize oxygen saturation on production of viable lumbar spinal slices from adult rats. The results show that the combined focus on reducing mechanical damage and maximizing tissue oxygenation greatly facilitates recording from lumbar motoneurons in adult rats. These procedures constitute a new protocol that makes it practical to study these uniquely important CNS neurons in vitro. Portions of this work have been reported in abstract form (Carp et al. 2007).

METHODS

Animals and preparation

All animal procedures were in accord with the *Guide for the Care and Use of Laboratory Animals* of the Institute of Laboratory Animal Resources, Commission on Life Sciences, National Research Council (National Academy Press, Washington, DC, 1996), and Department of Health, Education and Welfare Publication No. 0309-05377-3, *Guide for the Care and Use of Laboratory Animals* and were approved by the Wadsworth Center IACUC.

Experiments were conducted in 55 male rats (Sprague-Dawley, 147–513 g, 6–12 wk for 45 rats whose ages were known) using either the method previously described for preparing cervical spinal slices (Hori et al. 2001) (9 rats) or a new protocol built on the Hori method (the PEG protocol, described in the following text) (46 rats). For the former experiments, rats were anesthetized with pentobarbital (80 mg/kg, administered intraperitoneally [ip]), placed in a supine position, and perfused transcardially for 1 min with 100 ml of 2–4°C artificial cerebrospinal fluid (aCSF) in which NaCl had been replaced with sucrose (sucrose-aCSF) that contained (in mM): sucrose, 212.5; KCl, 3.5; NaHCO₃, 26; MgSO₄, 1.3; KH₂PO₄, 1.2; MgCl₂, 2.0; CaCl₂, 1.2; and glucose, 10 (298 mOsm). All aCSF solutions were bubbled with 95% O₂-5% CO₂.

After a dorsal laminectomy was performed, a loop of 5–0 silk suture was placed around the rostral end of the spinal cord and the

loose suture ends were attached to a manipulator. While constantly superfusing the spinal cord with 2–4°C sucrose-aCSF, the manipulator was gently raised to facilitate cutting the spinal cord and its roots in a rostral-to-caudal direction. After cutting the suture, the spinal cord was transferred in a plastic spoon filled with cold sucrose-aCSF to a dissection dish filled with 2–4°C sucrose-aCSF. The dura was removed and the spinal roots were cut as close to the cord as possible (long roots can interfere with slicing). The spinal cord was placed in a semicircular channel cut in a block of agar (Sigma, ~2 cm wide × 1.5 cm high × 1 cm thick) and covered with a second agar block. Then the assembly was glued (Loctite 404) to the platform of a vibrating microtome (Vibroslice, Campden or OTS-5000, FHC) and 450- μ m-thick transverse sections were cut in 2–4°C sucrose-aCSF. During slicing, the tissue was advanced at 0.25–0.30 mm/s and the blade (single- or double-edge carbon steel, Feather) oscillation frequency setting was 6–7 (Vibroslice, about 1,700–1,900 cycles/min) or 9–10 (OTS-5000).

The slices were incubated for 1 h at 34–36°C in normal-sodium aCSF, which consisted of (in mM): NaCl, 125; KCl, 3.5; NaHCO₃, 26; MgSO₄, 1.3; KH₂PO₄, 1.2; CaCl₂, 2.4; and glucose, 10 (294 mOsm). The slices were then transferred to mesh-floored holding chambers with normal aCSF at 29–31°C and remained there until used for recordings.

The PEG protocol is based on the preceding protocol, but has the following modifications. 1) The rats were anesthetized with ketamine: xylazine (80:10 mg/kg, ip). 2) The laminectomy was performed before (rather than after) the transcardiac perfusion. 3) The rats received 100% oxygen by mask throughout the laminectomy and continuing up until the transcardiac perfusion. 4) Just prior to perfusion, the rat was carefully turned from a prone to a supine position and the exposed spinal cord was positioned over a small well in the dissection surface filled with 2–4°C sucrose-aCSF to begin chilling the spinal cord and protect it from mechanical damage. 5) In preparation for slicing, the spinal cord was removed from the dissection dish, blotted on a premoistened piece of filter paper, and suspended within a short glass cylinder (13 mm high × 7 mm ID) in a 2–4°C sucrose-aCSF-filled stainless steel bath) while warm low-gelling-temperature agarose (~28°C, Sigma Type IX-A, 6% in sucrose-aCSF) was injected around it with a 1-ml syringe. The glass cylinder was removed from the bath after the agar hardened (~15 s). The agarose-embedded cord was partially ejected by applying gentle pressure with a 1-ml syringe plunger to allow excess agarose to be trimmed with a razor blade to within 1 mm of the cord, and then completely ejected directly onto a small drop (~10–12 μ l) of glue (Loctite 404) on the mounting platform of the vibrating microtome. A

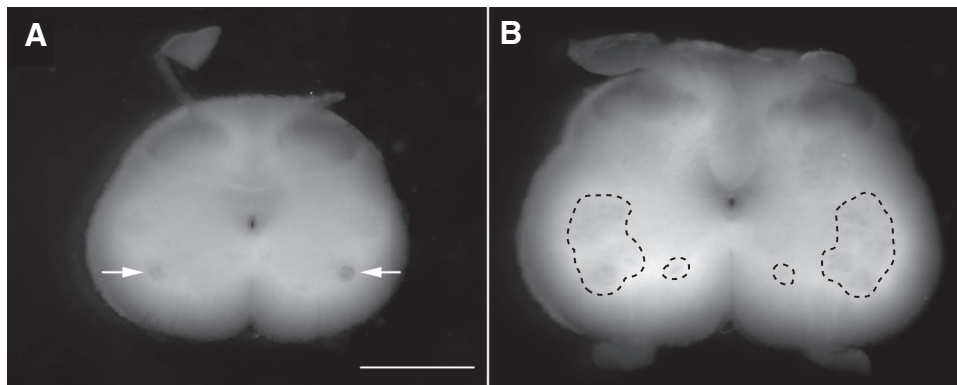


FIG. 1. Transverse 450- μ m-thick slices from the spinal cord 6.8 mm caudal (A) and 3.7 mm caudal (B) to the widest part of the lumbar enlargement of a 190-g (~6-wk-old) rat. The more caudal slice (A) contains a bilateral pair of dark circular regions (arrows) in the ventral horns (ventral toward bottom of picture) that correspond to the dorsolateral cell group in L5–L6 that contains pudendal motoneurons (McKenna and Nadelhaft 1986; Schroder 1980). This cell group is evident (but less prominent) in one slice rostral and 2 slices caudal to the one shown, but not beyond this region. In more rostral slices (e.g., B), irregularly shaped and usually less intensely dark motoneuron columns are evident throughout the ventral horn (circumscribed by dashed lines). Motoneurons recorded in these L4–L5 regions are likely to innervate hindlimb muscles. Scale bar = 1 mm.

14-mm-high \times 10-mm-wide Teflon block at the end of the mounting platform opposite the microtome blade prevented the agarose (which was glued directly in front of it) from bending or being dislodged during cutting. 6) Immediately after cutting, each slice was incubated for 60 s in PEG (30% wt/vol in distilled water, 870 mOsm; Sigma $M_n = 1,900\text{--}2,200$) (with fresh solution for each slice using 12-well tissue-culture trays) and was then rinsed for 1 min in normal aCSF at 34–36°C twice immediately prior to a 1-h incubation in normal aCSF at 34–36°C. The choice of a 60-s PEG incubation was guided by preliminary studies in nine animals (rats and mice) that failed to produce any acceptable recordings using 45-, 90-, or 120-s exposures (although acceptable recordings were obtained in two of three mouse experiments using a 75-s incubation).

Data collection and analysis

Each slice to be studied was transferred to the recording chamber, held on a mesh platform by harp-shaped silver wires with elastic threads, and superfused with normal aCSF at 3 ml/min at 29–31°C. Intracellular impalements were made with 30- to 60-M Ω long-taper electrodes or with 9- to 20-M Ω rapid-taper (“bee-stinger”) electrodes filled with 3 M potassium acetate. Data were recorded (Dagan 8700), low-pass filtered at 3–10 kHz, sampled at 6–20 kHz, and stored using WinWCP (Strathclyde Electrophysiology Software), and were analyzed using custom software. Impalements typically lasted 10–20 min (median recording time after stabilization was 9 min, with 10% of cells recorded for 20–90 min).

Hyperpolarizing 40-ms current pulses were used to evaluate input resistance and membrane time constant. Action potentials were elicited by short (0.6- to 1.0-ms) depolarizing current pulses (Fig. 2*B*, left panels) and/or by antidromic activation by stimulation with a Teflon-insulated silver wire electrode (0.125-mm diameter, \sim 100- μ m exposed tip) placed on the ventral root stub (Fig. 2*A*). Action potential amplitude was calculated as the difference between the peak of the action potential and the average resting potential during the 5 ms prior to stimulation. Afterhyperpolarization (AHP) duration, amplitude, and half-time (i.e., time from AHP maximum amplitude until recovery to half-maximal amplitude) were determined from action potentials elicited by the short current pulses. Long (40-ms) depolarizing current

pulses were used to determine rheobase (i.e., current at which probability of firing is 50%). The difference in amplitude between action potentials elicited by long and short depolarizing pulses determined the threshold depolarization (i.e., the depolarization from resting potential needed to reach the voltage threshold for action potential initiation (Carp 1992; Gustafsson and Pinter 1984; see Fig. 2*B*). Voltage threshold was calculated as the sum of the depolarization threshold and the resting membrane potential. Slow triangular current ramps (0.2–2.0 nA/s for 5 s in each direction) were used to induce repetitive firing. Repetitive firing behavior was characterized by the instantaneous firing rates and the currents at the onset and offset of repetitive firing.

Motoneuron labeling

Two rats received intramuscular injections of cholera toxin subunit-B conjugated to Alexa 594 and/or to fluorescein isothiocyanate (FITC; Invitrogen; 1–2 μ g/ μ l solution in sterile saline) to retrogradely label gastrocnemius and soleus motoneuron pools. Under ketamine–xylazine anesthesia (as described earlier), the skin of the lateral aspects of the lower hindlimbs was incised and the lateral and medial gastrocnemius and soleus muscles were exposed. Using a 100- μ l syringe with a 31-gauge needle under direct observation with a dissection microscope, the gastrocnemius muscles were injected slowly with 50–110 μ g of label divided among three injection tracks and soleus muscles were injected with 20–40 μ g of label divided between two injection tracks. After injection, the needle was withdrawn gradually over 3 min. After the injection site and surrounding tissues were flushed thoroughly with sterile saline, the incision was infiltrated with bupivacaine, closed with wound clips, and dressed with nitrofurazone. Three or 4 days after injection, spinal slices were prepared according to the PEG protocol.

Statistics

Statistical analyses of continuous variables used the *t*-test. Analysis of preparation success versus failure used the maximum likelihood chi-square test.

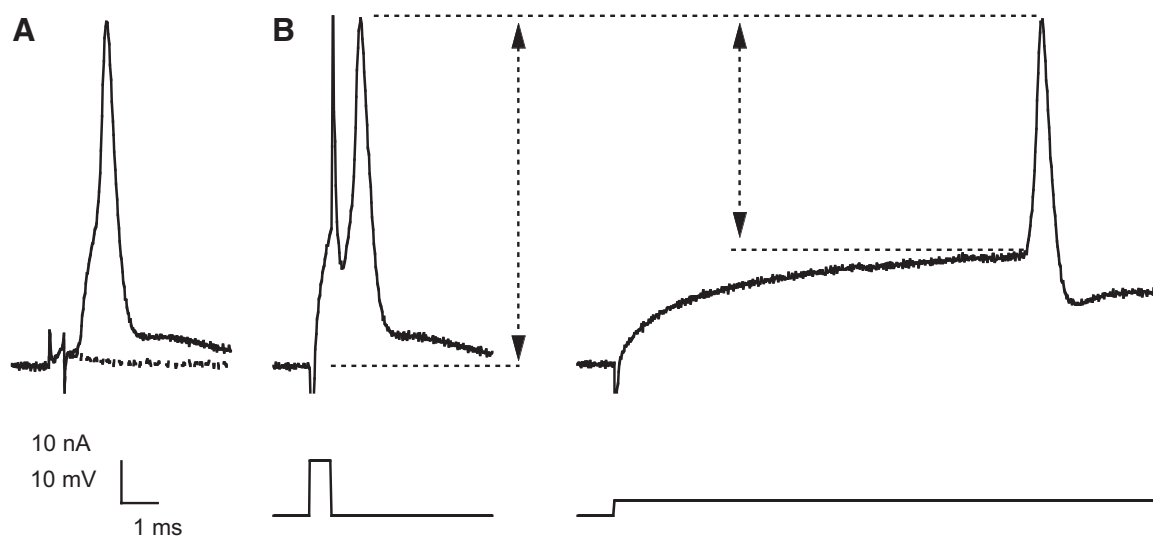


FIG. 2. Examples of action potentials (APs) elicited in motoneurons. *A*: membrane potential traces show that antidromic stimulation of the ventral root at just-threshold intensity elicits (solid line) or fails to elicit (dashed line) an AP. Resting potential, -61.7 mV. *B*: membrane potential (top traces) recorded during current injections (bottom traces) for the same motoneuron as in *A* (voltage traces in *A* and *B* are shown with the same absolute voltage level and scaling factor). Starting from similar resting potentials [-61.7 mV (left) and -61.3 mV (right)]; average membrane potential shown as bottom dashed horizontal line], just-threshold short (left) or long (right) depolarizing current pulses elicit APs with peaks that are similar to each other (top horizontal dashed line) and to that of the antidromic AP in *A*. The amplitude of each AP is indicated by vertical double-headed arrows. The difference between these 2 amplitudes defines the threshold depolarization (i.e., depolarization from the resting potential required to reach the voltage threshold for AP initiation).

RESULTS

Study design and data pool

Intracellular current-clamp recordings were made with sharp electrodes in transverse slices of lumbar spinal cord of adult rats from 105 neurons with action potential amplitudes ≥ 60 mV, which was the minimum value for acceptance into the data pool. Nine of them were tested by antidromic activation and were positively identified as motoneurons (see example in Fig. 2A). The rest of these neurons were presumed to be motoneurons because: 1) they were located in dark patches of the ventrolateral gray matter consistent with motor columns, 2) they had properties similar to those of the antidromically identified motoneurons (e.g., input resistance = 7.3 ± 3.8 vs. 7.8 ± 4.9 M Ω ; rheobase = 2.9 ± 0.8 vs. 3.1 ± 2.6 nA for antidromic motoneurons vs. other neurons, respectively), and 3) their input resistances were all substantially lower and their rheobases were all higher than the expected range of values for spinal interneurons capable of repetitive firing (Theiss and Heckman 2005).

Three measures were used to evaluate the success of each preparation: 1) the percentage of experiments that were successful, i.e., yielding at least one motoneuron meeting the acceptance criterion; 2) the average number of accepted motoneurons studied per experiment; and 3) the average action potential amplitude of the accepted motoneurons.

Motoneuron viability with the PEG protocol

The PEG protocol reliably produced slices with viable motoneurons. Recordings were attempted in a median of four slices per preparation. Neuronal impalements were obtained in 56% of the slices in which recording was attempted. The PEG protocol produced viable slices in 42 of 46 preparations (96%; three to five viable slices in 11 preparations, two in 17 preparations, and one in 14 preparations). It produced at least one acceptable (i.e., action potential ≥ 60 mV) motoneuron recording per preparation in 35 of 46 preparations (76%). The average number of acceptable motoneurons recorded per preparation was $2.15 (\pm 0.30$ SE) and the average action potential amplitude per successful preparation was $75.7 (\pm 1.1)$ mV. These results clearly demonstrate the reliability, yield, and recording quality achieved by the PEG protocol.

In contrast, application of the previously reported method for cervical spinal cord slices (Hori et al. 2001) resulted in successful recordings in two of nine experiments (22%; different from PEG protocol, $P = 0.009$ by chi-square test), and an average of $0.44 (\pm 0.29$ SE) recordings per experiment (different from PEG protocol, $P = 0.0016$ by t -test) with an average action potential amplitude of $61.3 (\pm 1.3)$ mV (different from PEG protocol, $P = 0.016$ by t -test). These action potential amplitudes are comparable to those from some recordings illustrated in Hori et al. (2001).

Factors affecting success

For the PEG protocol studies, the dissection time (i.e., the time from starting the thoracotomy until the first slice was cut) of successful preparations (range 8.4–12.5 min, median 11.0 min for 13 preparations in which this was measured) was not significantly different from that of unsuccessful preparations

(range 10.3–21.0 min, median 11.5 min; $P = 0.27$, Wilcoxon rank-sum test). Also, dissection time did not linearly predict the number of motoneurons studied per preparation ($P = 0.45$ by linear regression). Still, it should be noted that all preparations with at least three motoneurons studied had dissection times of ≤ 12.5 min.

Preparation success did not depend on body weight or age. Body weight (which was used as a covariant of age because data on animal age were incomplete) did not account for a significant amount of the variation in the outcome variables (least-squares fit, $P > 0.9$ for weight for both the number of motoneurons studied per preparation and their average action potential amplitude).

Results with the PEG protocol improved with repeated performance. Only 6 of the first 10 preparations were successful, whereas all of the final 10 preparations were successful ($P = 0.01$ by chi-square test). The average number of motoneurons recorded per preparation increased from $1.20 (\pm 0.49$ SE) for the first 10 preparations to $2.50 (\pm 0.27)$ for the last 10 preparations ($P = 0.03$ by t -test). Average action potential amplitude per successful preparation increased from $69.1 (\pm 2.5)$ mV for the first 10 preparations to $76.2 (\pm 1.4)$ mV for the last 10 preparations ($P = 0.02$ by t -test).

Motoneuron location and identity

Using the PEG protocol, recordings were made from 101 lumbar motoneurons, of which 64 were putative pudendal motoneurons and 37 were putative hindlimb motoneurons. The putative pudendal motoneurons were recorded from characteristic round dark regions in the lateral gray matter of the ventral horn (arrows in Fig. 1A). These areas probably represent dendritic bundles and cell bodies of pudendal motoneurons in caudal L5–L6 that innervate external urethral sphincter muscles (and ischiocavernosus in males) (McKenna and Nadelhaft 1986; Schroder 1980).

The putative hindlimb motoneurons were typically recorded from one to eight slices (0.45–3.6 mm) rostral to the pudendal motoneuron slices. They were located throughout the motor columns of the ventral horn, which are less intensely dark and more irregularly shaped (indicated by dotted outlines in Fig. 1B) than the pudendal motoneuron region. Their location rostral to the putative pudendal motoneurons indicates that they are mainly L4–L5 hindlimb motoneurons (Nicolopoulos-Stouraras and Iles 1983). This identification is also supported by observations in two rats in which gastrocnemius and soleus muscles were injected with fluorescently labeled cholera toxin. The labeled motoneurons were concentrated in the same central and lateral ventral gray matter areas from which the putative hindlimb motoneurons were recorded. No labeled motoneurons were found in the more caudal location of the putative pudendal motoneurons.

Four additional motoneurons were recorded from cervical slices in the nine preparations that used the protocol of Hori et al. (2001). The recordings targeted the small gray irregularly shaped clusters in the mid- to lateral-ventral horn that form the motoneuron columns of forelimb and phrenic motoneurons.

Motoneuron properties

From the 101 lumbar motoneurons with action potentials ≥ 60 mV, we recorded responses of 92 motoneurons to a

TABLE 1. *Properties of hindlimb and pudendal motoneurons*

Property	Motoneuron	
	Hindlimb	Pudendal
Resting potential, mV	-66.9 ± 12.3	-59.8 ± 9.2**
AP amplitude, mV	78.7 ± 8.9	77.2 ± 7.9
Input resistance, mΩ	5.1 ± 3.4	9.2 ± 4.8***
Time constant, ms	3.6 ± 2.3	4.4 ± 2.0
AHP duration, ms	45.5 ± 12.8	47.6 ± 11.2
AHP half-time, ms	17.2 ± 7.0	18.6 ± 5.8
AHP amplitude, mV	-3.0 ± 2.0	-4.3 ± 3.1*
Rheobase, nA	4.3 ± 3.0	2.4 ± 1.9**
Threshold depolarization, mV	18.2 ± 7.5	17.5 ± 6.5
Number of cells	32–35	49–57

Values are means ± SD. See text for motoneuron identification criteria. Amplitude of action potential (AP) elicited by brief [0.4- to 1.3-ms (typically 0.6-ms) current pulse]. Threshold depolarization from resting potential required to elicit AP. **P* < 0.05, ***P* < 0.01, and ****P* < 0.001, different from hindlimb motoneurons by *t*-test.

series of rectangular current pulse injection protocols for determination of input resistance, time constant, current threshold (rheobase), and voltage threshold, and to triangular current ramps for determination of repetitive firing properties.

Table 1 summarizes the properties of hindlimb and pudendal motoneurons. Hindlimb motoneurons have lower input resistance and higher rheobase than do pudendal motoneurons, which is consistent with the fact that pudendal motoneurons are smaller (Chen and Wolpaw 1994; Collins 3rd et al. 1992). Resting potential is more hyperpolarized in hindlimb than in pudendal motoneurons. These relationships are unlikely to reflect differences in impalement quality (since input resistance is lowest in hindlimb motoneurons, which have the largest action potentials and most negative resting potentials) and thus these observations probably reflect true physiological differences between hindlimb and pudendal motoneurons.

Table 2 compares the properties of rat hindlimb motoneurons recorded in vitro (i.e., present data) and in vivo (Button

et al. 2006). Motoneurons recorded in vivo (right columns of Table 2) display a systematic distribution of properties in which those innervating fast-twitch muscle (fast motoneurons) tend to have higher rheobase, lower input resistance, and shorter AHP duration than do those innervating slow-twitch muscle (slow motoneurons) (Burke 1981). The same pattern is seen in vitro, where fast motoneurons (distinguished from slow motoneurons by their AHP half-time; Gardiner 1993) have significantly lower rheobases, higher input resistances, and smaller AHP amplitudes than do slow motoneurons.

When triangular current ramps were injected, motoneurons recorded in vitro behaved like motoneurons recorded in vivo (Button et al. 2006): they were recruited during the ascending current ramp, fired repetitively, and then were derecruited during the descending current ramp (Fig. 3). Firing behavior was quantified by the instantaneous firing rates (calculated from the interspike intervals) and the currents at the onset and offset of firing. Ramp onset and offset firing rates and currents were significantly higher in fast than in slow motoneurons in vitro, as they are in vivo (Table 2). The difference between offset and onset currents was significantly different between fast and slow motoneurons in vitro, but not in vivo (although the latter displayed a similar trend).

During triangular current ramps, all motoneurons recorded in vitro exhibited one of two characteristic response patterns. One pattern was higher offset firing rate and offset current than onset firing rate and onset current (i.e., offset minus onset is positive; Fig. 3, *A*, *C*, *E*, and *G*). The other pattern was lower offset firing rate and current than onset firing rate and current (i.e., offset minus onset current is negative; Fig. 2, *B*, *D*, *F*, and *H*). These response patterns are comparable to the “adaptive” and “linear-plus-sustained” firing patterns, respectively, described for rat motoneurons in vivo (Button et al. 2006). The linear-plus-sustained pattern is more frequently expressed in slow (8/14; 57%) than in fast (7/28; 25%) hindlimb motoneurons recorded in vitro (*P* = 0.04, chi-square test).

TABLE 2. *Comparison of rat hindlimb motoneuron properties recorded in vitro and in vivo*

Property	In Vitro		In Vivo	
	Fast	Slow	Fast	Slow
Resting potential, mV	-68 ± 11	-63 ± 14	-71 ± 6	-64 ± 6
AP amplitude, mV	79.9 ± 8.9	75.7 ± 8.6	76.0 ± 11.5	82.6 ± 12.2
Input resistance, mΩ	4.0 ± 2.1**	7.7 ± 4.8	1.8 ± 0.6	2.7 ± 1.2
AHP half-time, ms	14 ± 3***	27 ± 4	14 ± 2	27 ± 7
AHP amplitude, mV	-2.4 ± 1.2*	-4.5 ± 2.8	-1.5 ± 1.1	-2.7 ± 1.2
Rheobase, nA	4.9 ± 3.2*	2.8 ± 1.5	9.8 ± 3.0	5.9 ± 4.7
Voltage threshold, mV	-51 ± 12	-46 ± 9	-52 ± 7	-46 ± 12
Ramp onset firing rate, pps	16.7 ± 6.6**	9.2 ± 1.1	26.5 ± 7.7	16.7 ± 7.2
Ramp offset firing rate, pps	12.5 ± 3.6*	8.8 ± 2.6	24.7 ± 6.8	14.1 ± 5.6
Ramp onset firing current, nA	7.9 ± 4.6**	2.8 ± 1.8	26.5 ± 7.7	16.7 ± 7.2
Ramp offset firing current, nA	8.2 ± 4.9**	2.5 ± 1.6	10.9 ± 3.1	7 ± 4
Offset – onset current, nA	0.3 ± 0.8***	-0.3 ± 0.2	-0.2 ± 0.6	-0.4 ± 0.3
Number of motoneurons	15–26	6–10	21	7

Values are means ± SD. In vivo data are from Table 1 of Button et al. (2006), except for the action potential (AP) amplitude data, which are calculated from 216 motoneurons pooled from Table 1 of Beaumont and Gardiner (2003) and Table 1 of Cormery et al. (2005). Fast motoneurons are defined by AHP half-time <20 ms; asterisks indicate significant differences from slow motoneurons at **P* < 0.05, ***P* < 0.01, and ****P* < 0.001. Slow motoneurons are defined by AHP half-time ≥20 ms. With respect to rheobase, the current threshold for AP initiation is during 40-ms depolarizing pulse. The instantaneous firing rate (ramp onset) from the first interspike interval (ISI) is that during the ascending current ramp. The instantaneous firing rate (ramp offset) from the last ISI is that during the descending current ramp. Ramp onset current is that during the ascending ramp at which firing begins. Ramp offset current is that during the descending ramp at which firing ends: Offset – onset current is the ramp current at firing offset minus the ramp current at firing onset.

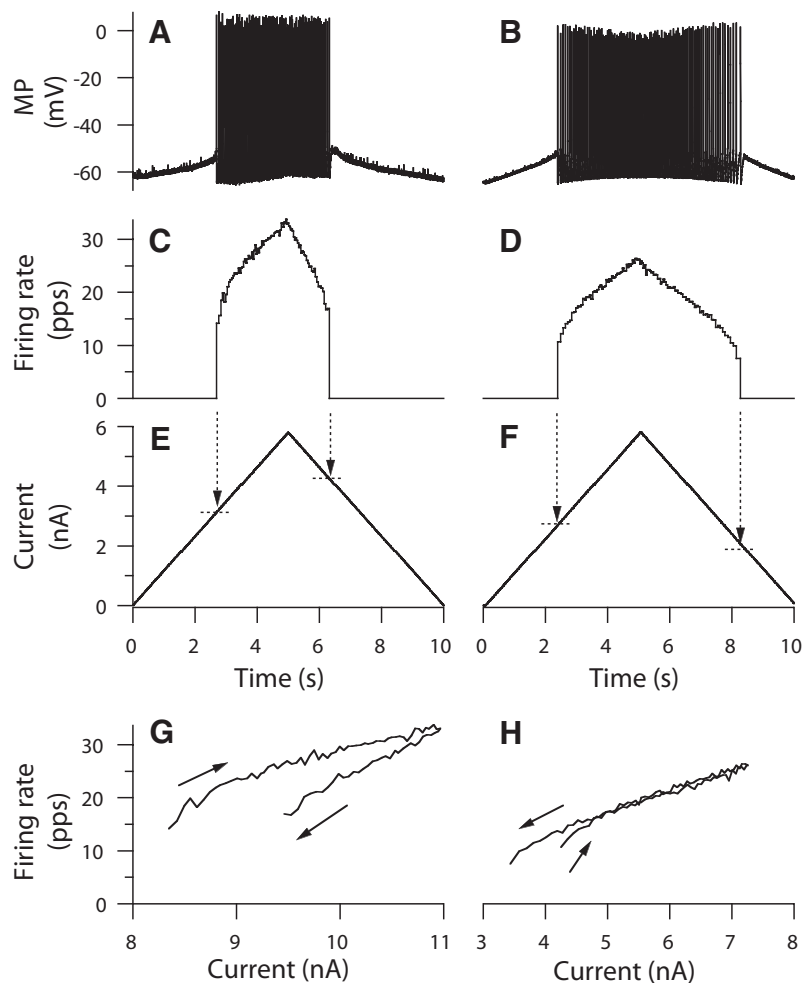


FIG. 3. Examples of 2 types of repetitive firing behavior in response to injected current. Membrane potential (MP) (A, B) and instantaneous firing rate in pulses per second (pps) (C, D) are shown during triangular ramp current injections (E, F) as a function of time. Dashed vertical arrows indicate recruitment and derecruitment times; dashed horizontal lines indicate recruitment and derecruitment current levels (E, F). A DC bias current of +5.6 nA is applied to the motoneuron on the left and +1.9 nA to the motoneuron on the right throughout the triangular ramp current (not included in current traces in E and F). The current–rate relationships (G, H) reveal the time course of the change in instantaneous firing rate during the rising and falling legs of the triangular ramp current (firing sequence starting at recruitment and ending at derecruitment indicated by upward-pointing and downward-pointing arrows, respectively). The left panels (A, C, E, and G) illustrate a type of firing behavior in which the current and firing rate at which this motoneuron is recruited are lower than the current and firing rate at which it is derecruited. This is expressed as clockwise hysteresis (as indicated by the arrows) in the current–rate plot (G). The right panels (B, D, F, and H) illustrate a different type of firing behavior in which the current and firing rate at which this motoneuron is recruited are higher than the current and firing rate at which it is derecruited. This is expressed as a counterclockwise hysteresis at the beginning and end (arrows) of the current–rate plot (H).

DISCUSSION

This report describes a new protocol for performing intracellular recording from motoneurons in lumbar transverse spinal slices from adult rats. The five features of the PEG protocol that distinguish it from the methodology on which it is based (Hori et al. 2001) are: 1) incubation of slices in PEG, 2) performing the laminectomy prior to transcardiac perfusion, 3) exposure to 100% oxygen prior to transcardiac perfusion, 4) anesthesia with ketamine/xylazine, and 5) embedding the spinal cord in agar before slicing. Together, these procedures routinely produced lumbar spinal slices in which motoneurons were recorded with action potentials of 60–90 mV.

The validity of the PEG protocol is indicated by the close similarities between the motoneuron data it has produced and data from motoneurons studied *in vivo*. These similarities include 1) hindlimb motoneurons have lower input resistance and higher rheobase than those of pudendal motoneurons in both *in vivo* data (Burke 1981; Hochman et al. 1991; Sasaki 1991) and our *in vitro* data; 2) rat motoneurons display comparable patterns of type-dependent (i.e., fast vs. slow) differences in rheobase, input resistance, AHP amplitude, and repetitive firing onset and offset rates and currents in both *in vivo* data (Burke 1981; Button et al. 2006) and our *in vitro* data; 3) the two dominant types of motoneuron repetitive firing behavior (i.e., adaptive and linear-plus-sustained firing) seen in

our *in vitro* data (Fig. 3) are also seen in previously reported *in vivo* data (Button et al. 2006); 4) the linear-plus-sustained repetitive firing behavior we found *in vitro* probably reflects a persistent inward current that is well characterized in motoneurons *in vivo* (Heckmann et al. 2005); and 5) firing patterns indicative of an underlying inward persistent current are more frequently evident in slow than in fast motoneurons in both *in vivo* data (Button et al. 2006) and our *in vitro* data.

The modest quantitative differences in rat lumbar motoneuron properties between *in vivo* data (Button et al. 2006) and our *in vitro* data probably reflect differences in synaptic inputs to the motoneurons rather than differences in motoneuron intrinsic properties. That input resistance is lower and rheobase is higher *in vivo* than *in vitro* is unlikely to reflect a lower impalement quality (due to the mechanical instability inherent to *in vivo* recording) because action potential amplitude and resting potential (which should also be adversely affected by poor impalements) are comparable *in vivo* and *in vitro* (Table 2). Rather, these observations probably reflect greater synaptic drive to motoneurons *in vivo* than *in vitro*. Similarly, the observation that rat motoneurons display lower firing rates and less firing-rate hysteresis during ascending and descending current ramps *in vitro* than *in vivo* (Button et al. 2006) probably reflects the reduction *in vitro* of neuromodulatory influences on the persistent inward currents that control repetitive firing behavior (Heckmann et al. 2005).

Although the PEG protocol produces recordings from lumbar motoneurons in vitro with action potential amplitudes comparable to those in vivo (Table 2; Beaumont and Gardiner 2003; Cormery et al. 2005), Harvey et al. (2006) report larger action potentials recorded from sacrocaudal motoneurons in vitro (i.e., average action potential amplitude of 92.0 mV and average overshoot of 19.3 mV). This difference could reflect an intrinsic difference between lumbar and sacrocaudal motoneurons. It could also reflect the deleterious effect of slicing (the sacrocaudal preparation is isolated, but unsectioned) and/or differences in viability in vitro between lumbar and sacrocaudal motoneurons. In any case, the PEG protocol might be further improved. Possible modifications include parasagittal (instead of transverse) slicing to take advantage of the motoneurons' smaller mediolateral than rostrocaudal dendritic extent (Chen and Wolpaw 1994), replacing the warm agarose embedding medium with a cold photocured hydrogel to reduce spinal cord heat exposure, and preconditioning to improve motoneuron resistance to hypoxia and ischemia (Sharp et al. 2004; Steiger and Hanggi 2007).

Consideration of the mechanisms of the key features of the PEG protocol provides insight into the efficacy of their addition to the slice preparation protocol. PEG fuses lipid membranes by excluding water from the lipid interface (Lentz 2007). It fuses the cut ends of peripheral nerves and reestablishes axonal conduction (Lore et al. 1999; Shi et al. 1999) and, in a model of spinal cord injury, it protects central neurons by making them less leaky (Shi and Borgens 2000). In the present context, PEG may fuse freshly transected dendrites at the slice surfaces, thereby preventing the ionic imbalance that would otherwise result from these large transmembrane shunts. If this hypothesis is correct, PEG application is the only treatment that directly promotes sealing of the neuronal elements cut during slice preparation. In addition, PEG incubation could be incorporated into slice protocols for other CNS tissue in which the target neuron's extensive dendritic arborization puts it at risk of damage during sectioning (e.g., Davies et al. 2007).

Some of the other distinctive features of the PEG protocol address the motoneuron's responses to the ischemic/hypoxic insult (Acker and Acker 2004; Krnjevic 1999) that begins at the onset of the thoracotomy immediately before transcardiac perfusion. Prior exposure to 100% oxygen (as used in an in vitro preparation of the sacrocaudal spinal cord; Li and Bennett 2003) maximizes tissue oxygen saturation (which may be compromised by anesthesia). Performing the laminectomy prior to the perfusion shortens by ≥ 2 min the period of hypoxia/ischemia that occurs before the spinal cord is fully cooled. Additionally, performing the laminectomy prior to the perfusion allows the laminectomy to be performed more slowly, thereby reducing the risk of damaging the spinal cord. Anesthesia with the *N*-methyl-D-aspartate receptor antagonist ketamine may reduce glutamatergic excitotoxic damage (Albensi 2007).

Embedding the spinal cord in warm agar followed by rapid cooling may help to further reduce mechanical trauma. Compared with using agar blocks (which require a precisely cut channel in which the spinal cord rests during slicing) (Hori et al. 2001), spinal cord embedding does not require manual shaping of the agar, reduces the potential for damage by tissue compression, and surrounds the spinal cord completely,

thereby providing integral support and decreasing the chance of the spinal cord being pulled out of the agar during slicing.

Our experimental design tested the efficacy of the PEG protocol as a whole, but did not assess the individual contributions of its components. Except for PEG, all of the other individual components have been used in other in vitro preparations (Carlin et al. 2000; Hirayama et al. 1988; Li and Bennett 2003; Takahashi 1978) and they presumably contribute to the efficacy of those protocols and of the current PEG protocol. Nevertheless, the fact that a protocol containing PEG is the only method described to date that produces reliable motoneuron recordings in lumbar slices from adult rats and the observation that its effect on slice viability depends on exposure time suggest that PEG makes the most important neuroprotective contribution to the protocol.

In summary, this study describes and validates a new protocol for studying lumbar motoneurons in spinal cord slices from adult rats. Ancillary studies indicate that this protocol is also applicable to adult mouse spinal cord (Carp et al. 2007). Rats and mice have rapidly become the models of choice for studies of normal and pathological motor function. The reliable in vitro preparation described here should foster physiological and pharmacological in vitro studies of motoneuron intrinsic properties and synaptic inputs. This new protocol should be particularly valuable for studying motoneuron plasticity during aging, after ischemic or traumatic injury to the brain or spinal cord, and in animal models of neurodegeneration.

ACKNOWLEDGMENTS

We thank Dr. Nobuaki Hori for providing training to J. S. Carp in performing the cervical spinal slice preparation; Dr. Richard Borgens for helpful comments on using polyethylene glycol with neural tissue; R. Cole (Advanced Light Microscopy Core of the Wadsworth Center) for assistance with collection and preparation of anatomical images; S. Meyer for construction of dissection and molding chambers and the recording platform; Drs. Mingchen Jiang and Dennis McFarland for thoughtful comments on this manuscript; and H. Sheikh for technical assistance in the early stages of this project.

GRANTS

This work was supported by National Institutes of Health Grants NS-22189 to J. R. Wolpaw and HD-36020 to X. Y. Chen.

REFERENCES

- Acker T, Acker H. Cellular oxygen sensing need in CNS function: physiological and pathological implications. *J Exp Biol* 207: 3171–3188, 2004.
- Albensi BC. The NMDA receptor/ion channel complex: a drug target for modulating synaptic plasticity and excitotoxicity. *Curr Pharm Des* 13: 3185–3194, 2007.
- Bagust J, Kerkut GA. An in vitro preparation of the spinal cord of the mouse. In: *Electrophysiology of Isolated Mammalian CNS Preparations*, edited by Kerkut GA, Wheal HV. London: Academic Press, 1981, p. 337–365.
- Beaumont E, Gardiner PF. Endurance training alters the biophysical properties of hindlimb motoneurons in rats. *Muscle Nerve* 27: 228–236, 2003.
- Bennett DJ, Li Y, Siu M. Plateau potentials in sacrocaudal motoneurons of chronic spinal rats, recorded in vitro. *J Neurophysiol* 86: 1955–1971, 2001.
- Berger AJ. Recent advances in respiratory neurobiology using in vitro methods. *Am J Physiol Lung Cell Mol Physiol* 259: L24–L29, 1990.
- Biscoe TJ, Duchon MR. Synaptic physiology of spinal motoneurons of normal and spastic mice: an in vitro study. *J Physiol* 379: 275–292, 1986.
- Brock LG, Coombs JS, Eccles JC. Action potentials of motoneurons with intracellular electrode. *Proc Univ Otago Med Sch* 29: 14–15, 1951.
- Brownstone R. Beginning at the end: repetitive firing properties in the final common pathway. *Prog Neurobiol* 78: 156–172, 2006.
- Burke RE. Motor units: anatomy, physiology and functional organization. In: *Handbook of Physiology. The Nervous System. Motor Control*. Bethesda, MD: Am. Physiol. Soc., 1981, sect. 1, vol. II, pt. 1, p. 345–422.

- Burke RE.** John Eccles' pioneering role in understanding central synaptic transmission. *Prog Neurobiol* 78: 173–188, 2006.
- Button D, Gardiner K, Marqueste T, Gardiner P.** Frequency–current relationships of rat hindlimb alpha-motoneurons. *J Physiol* 573: 663–677, 2006.
- Carlin KP, Jiang Z, Brownstone RM.** Characterization of calcium currents in functionally mature mouse spinal motoneurons. *Eur J Neurosci* 12: 1624–1634, 2000.
- Carp JS.** Physiological properties of primate lumbar motoneurons. *J Neurophysiol* 68: 1121–1132, 1992.
- Carp JS, Mongeluzi DL, Tennissen AM, Chen XY, Wolpaw JR.** Intracellular recordings from lumbar spinal motoneurons of adult rats and mice in vitro. Program No. 404.8. *2007 Abstract Viewer/Itinerary Planner*. Washington, DC: Society for Neuroscience, 2007. Online.
- Carp JS, Tennissen AM, Wolpaw JR.** Intracellular recording from adult mouse spinal motoneurons in vitro: methods development. Program No. 496.15. *2003 Abstract Viewer/Itinerary Planner*. Washington, DC: Society for Neuroscience, 2003. Online.
- Carriedo SG, Yin HZ, Weiss JH.** Motor neurons are selectively vulnerable to AMPA/kainate receptor-mediated injury in vitro. *J Neurosci* 16: 4069–4079, 1996.
- Chen XY, Wolpaw JR.** Triceps surae motoneuron morphology in the rat: a quantitative light microscopic study. *J Comp Neurol* 343: 143–157, 1994.
- Collins WF 3rd, Seymour A, Klugewicz S.** Differential effect of castration on the somal size of pudendal motoneurons in the adult male rat. *Brain Res* 577: 326–330, 1992.
- Cormery B, Beaumont E, Csukly K, Gardiner P.** Hindlimb unweighting for 2 weeks alters physiological properties of rat hindlimb motoneurons. *J Physiol* 568: 841–850, 2005.
- Davies ML, Kirov SA, Andrew RD.** Whole isolated neocortical and hippocampal preparations and their use in imaging studies. *J Neurosci Methods* 166: 203–216, 2007.
- Dingledine R, Dodd J, Kelly J.** The in vitro brain slice as a useful neurophysiological preparation for intracellular recording. *J Neurosci Methods* 2: 323–362, 1980.
- Duggal N, Lach B.** Selective vulnerability of the lumbosacral spinal cord after cardiac arrest and hypotension. *Stroke* 33: 116–121, 2002.
- Dunwiddie T, Mueller A, Basile A.** The use of brain slices in central nervous system pharmacology. *Fed Proc* 42: 2891–2898, 1983.
- Fulton BP.** Motoneurone activity in an isolated spinal cord preparation from the adult mouse. *Neurosci Lett* 71: 175–180, 1986.
- Gardiner PF.** Physiological properties of motoneurons innervating different muscle unit types in rat gastrocnemius. *J Neurophysiol* 69: 1160–1170, 1993.
- Gustafsson B, Pinter MJ.** An investigation of threshold properties among cat spinal alpha-motoneurons. *J Physiol* 357: 453–483, 1984.
- Harvey PJ, Li Y, Li X, Bennett DJ.** Persistent sodium currents and repetitive firing in motoneurons of the sacrocaudal spinal cord of adult rats. *J Neurophysiol* 96: 1141–1157, 2006.
- Heckmann CJ, Gorassini MA, Bennett DJ.** Persistent inward currents in motoneuron dendrites: implications for motor output. *Muscle Nerve* 31: 135–156, 2005.
- Hirayama T, Ono H, Fukuda H.** Unit activity of ventral horn cells in spinal cord slices isolated from adult rats. *Neurosci Lett* 91: 343–348, 1988.
- Hochman S, Fedirchuk B, Shefchyk S.** Membrane electrical properties of external urethral and external anal sphincter somatic motoneurons in the decerebrate cat. *Neurosci Lett* 127: 87–90, 1991.
- Hori N, Tan Y, King M, Strominger N, Carpenter D.** Differential actions and excitotoxicity of glutamate agonists on motoneurons in adult mouse cervical spinal cord slices. *Brain Res* 958: 434–438, 2002.
- Hori N, Tan Y, Strominger N, Carpenter D.** Intracellular activity of rat spinal cord motoneurons in slices. *J Neurosci Methods* 112: 185–191, 2001.
- Jiang Z, Rempel J, Li J, Sawchuk MA, Carlin KP, Brownstone RM.** Development of L-type calcium channels and a nifedipine-sensitive motor activity in the postnatal mouse spinal cord. *Eur J Neurosci* 11: 3481–3487, 1999.
- Kerkut GA, Bagust J.** The isolated mammalian spinal cord. *Prog Neurobiol* 46: 1–48, 1995.
- Krnjevic K.** Early effects of hypoxia on brain cell function. *Croat Med J* 40: 375–380, 1999.
- Lentz B.** PEG as a tool to gain insight into membrane fusion. *Eur Biophys J* 36: 315–326, 2007.
- Li Y, Bennett DJ.** Persistent sodium and calcium currents cause plateau potentials in motoneurons of chronic spinal rats. *J Neurophysiol* 90: 857–869, 2003.
- Lore AB, Hubbell JA, Bobb DS Jr, Ballinger ML, Loftin KL, Smith JW, Smyers ME, Garcia HD, Bittner GD.** Rapid induction of functional and morphological continuity between severed ends of mammalian or earthworm myelinated axons. *J Neurosci* 19: 2442–2454, 1999.
- McKenna K, Nadelhaft I.** The organization of the pudendal nerve in the male and female rat. *J Comp Neurol* 248: 532–549, 1986.
- Nicolopoulos-Stourmaras S, Iles JF.** Motor neuron columns in the lumbar spinal cord of the rat. *J Comp Neurol* 217: 75–85, 1983.
- Nohda K, Nakatsuka T, Takeda D, Miyazaki N, Nishi H, Sonobe H, Yoshida M.** Selective vulnerability to ischemia in the rat spinal cord: a comparison between ventral and dorsal horn neurons. *Spine* 32: 1060–1066, 2007.
- Rekling JC, Funk GD, Bayliss DA, Dong XW, Feldman JL.** Synaptic control of motoneuronal excitability. *Physiol Rev* 80: 767–852, 2000.
- Sasaki M.** Membrane properties of external urethral and external anal sphincter motoneurons in the cat. *J Physiol* 440: 345–366, 1991.
- Schroder H.** Organization of the motoneurons innervating the pelvic muscles of the male rat. *J Comp Neurol* 192: 567–587, 1980.
- Sharp FR, Ran R, Lu A, Tang Y, Strauss KI, Glass T, Ardizzone T, Bernaudin M.** Hypoxic preconditioning protects against ischemic brain injury. *NeuroRx* 1: 26–35, 2004.
- Shi R, Borgens R.** Anatomical repair of nerve membranes in crushed mammalian spinal cord with polyethylene glycol. *J Neurocytol* 29: 633–643, 2000.
- Shi R, Borgens R, Blight A.** Functional reconnection of severed mammalian spinal cord axons with polyethylene glycol. *J Neurotrauma* 16: 727–738, 1999.
- Steiger HJ, Hanggi D.** Ischaemic preconditioning of the brain, mechanisms and applications. *Acta Neurochir (Wien)* 149: 1–10, 2007.
- Takahashi T.** Intracellular recording from visually identified motoneurons in rat spinal cord slices. *Proc R Soc Lond B Biol Sci* 202: 417–421, 1978.
- Theiss RD, Heckman CJ.** Systematic variation in effects of serotonin and norepinephrine on repetitive firing properties of ventral horn neurons. *Neuroscience* 134: 803–815, 2005.
- Ulfhake B, Kellerth JO.** A quantitative light microscopic study of the dendrites of cat spinal alpha-motoneurons after intracellular staining with horseradish peroxidase. *J Comp Neurol* 202: 571–583, 1981.
- von Lewinski F, Keller B.** Ca²⁺, mitochondria and selective motoneuron vulnerability: implications for ALS. *Trends Neurosci* 28: 494–500, 2005.